

BCS - BEC crossover at $T = 0$: A Dynamical Mean Field Theory Approach

Arti Garg,¹ H. R. Krishnamurthy,² and Mohit Randeria³

¹*Department of Theoretical Physics, Tata Institute of Fundamental Research, Mumbai 400 005, India*

²*Centre for Condensed Matter Theory, Department of Physics,
Indian Institute of Science, Bangalore 560 012, India ,*

and Condensed matter Theory Unit, JNCASR, Jakkur, Bangalore 560 064, India

³*Department of Theoretical Physics, Tata Institute of Fundamental Research, Mumbai 400 005, India;*

Department of Physics, The Ohio State University, Columbus, OH 43210

We study the $T = 0$ crossover from the BCS superconductivity to Bose-Einstein condensation in the attractive Hubbard Model within dynamical mean field theory (DMFT) in order to examine the validity of Hartree-Fock-Bogoliubov (HFB) mean field theory, usually used to describe this crossover, and to explore physics beyond it. Quantum fluctuations are incorporated using iterated perturbation theory as the DMFT impurity solver. We find that these fluctuations lead to large quantitative effects in the intermediate coupling regime leading to a reduction of both the superconducting order parameter and the energy gap relative to the HFB results. A qualitative change is found in the single-electron spectral function, which now shows incoherent spectral weight for energies larger than three times the gap, in addition to the usual Bogoliubov quasiparticle peaks.

1. INTRODUCTION

The problem of the crossover from BCS superconductivity to Bose-Einstein Condensation (BEC) of composite bosons, where the superconducting coherence length (roughly the size of the fermion pair binding) is respectively much larger than or much smaller than the average inter-fermion spacing, has been a problem of great interest from the very early stages of development of the theory of superconductivity. It was first addressed in the very early work of Eagles [1]. In 1980 Leggett [2] showed, using a variational approach, that at zero temperature the superconducting BCS ground state at weak coupling evolves smoothly into a Bose condensate state of tightly bound "molecules" at strong coupling. Nozières and Schmitt-Rink [3] extended the analysis to lattice models and to finite temperature and showed that the transition temperature T_c between the normal and the superconducting state evolves continuously as a function of the magnitude of the attractive interaction between the fermions. The discovery of high T_c superconductors, which are characterized by short coherence length comparable to (but larger than) the inter-particle spacing, led to a resurgence of interest in the BCS-BEC crossover. A variety of interpolation schemes between weak and strong coupling developed using variational methods, functional integrals, and diagrammatic methods have been explored [4, 5, 6], and the existence of pseudo-gap anomalies in the normal state of a short coherence length superconductor has been established in two-dimensional systems [7, 8]. Recently it has become possible to directly realize the BCS-BEC crossover in a dilute atomic gas of Fermions in a trap, by varying their two-body interaction (scattering length) using a Feshbach resonance [9].

In this paper we analyze the BCS-BEC crossover in the attractive Hubbard model using the dynamical mean

field theory (DMFT) [10, 11] approach. Our goal is to focus on the intermediate coupling regime $U/t \approx 1$ where one has no obvious small parameter. Since the DMFT becomes exact in the limit of infinite dimensions [10, 11], we are, in a sense, using the inverse coordination number of the lattice as the small parameter. The attractive Hubbard model has been studied recently using DMFT, but primarily in the normal phase [12] to analyze pair formation above T_c and related phenomena. We focus here on the superconducting phase at zero temperature, in part because the DMFT method has been much less explored in broken symmetry phases.

The remainder of the paper is organized as follows. In Section 2, we define the model and review the Hartree-Fock-Bogoliubov (HFB) mean field theory. In Section 3, we briefly summarize the DMFT approach in the superconducting (SC) state and then describe the specific implementation of DMFT which we use, namely the iterated perturbation theory (IPT), in Section 4. In Section 5 we present our results for the chemical potential, energy gap, SC order parameter, density of states, spectral function, occupation probability and superfluid stiffness. We discuss how each of these evolves from the weak coupling BCS limit to the strong coupling BEC limit, and to what extent the quantum fluctuations included in the DMFT implemented using IPT modify the results relative to HFB mean field theory.

2. MODEL

We use the simplest lattice model which exhibits the BCS-BEC crossover, defined by the Hamiltonian

$$H = -t \sum_{ij,\sigma} c_{i\sigma}^\dagger c_{j\sigma} - |U| \sum_i n_{i\uparrow} n_{i\downarrow} - \mu \sum_i n_i \quad (1)$$

The first term describes the kinetic energy of fermions with nearest neighbor hopping t , the on-site attractive interaction ($-|U|$) induces s-wave, singlet pairing and leads to a superconducting ground state for all $n \neq 1$, with the chemical potential μ determining the filling factor n . (We will not study the system with $n = 1$ for which superconducting and charge-density wave orders coexist).

The simplest mean-field description of this system uses the Hartree-Fock-Bogoliubov (HFB) theory leading to the following self-consistent equations for the “gap” Δ and μ at a temperature $T \equiv 1/(k_B\beta)$:

$$\frac{1}{|U|} = \sum_k \frac{\tanh(\beta E_k/2)}{2E_k} \quad (2)$$

and

$$n = 2 \sum_k \left[1 - \frac{\xi_k}{E_k} \tanh\left(\frac{\beta E_k}{2}\right) \right]. \quad (3)$$

We use standard notation where ϵ_k is the band dispersion for the fermions and $E_k = \sqrt{\Delta^2 + \xi_k^2}$ with $\xi_k \equiv \epsilon_k - \mu - |U|n/2$. As is well known [4, 5, 6, 13] at $T = 0$ the solution of these equations leads to a BCS superconductor in the weak coupling $|U|/t \ll 1$ limit, to a BEC of hard core bosons in the opposite extreme $|U|/t \gg 1$, and interpolates smoothly in between. However, the finite temperature solutions of these equations for $|U|/t \gg 1$ yields a $T_c \sim |U|$, not the BEC transition temperature scale expected to be of order $t^2/|U|$, and the HFB approach therefore does not constitute an interpolating approximation at finite T [4].

The DMFT is one of the simplest schemes that has the potential to overcome some of these limitations of simple HFB theory. As we discuss in the following sections, the lattice dependence of quantities that arise in the DMFT is not via the momentum k but only via the band dispersion ϵ_k , and hence we can make the replacement

$$\sum_k \rightarrow \int d\epsilon \rho(\epsilon), \quad (4)$$

where $\rho(\epsilon)$ is the (bare) band density of states(DOS). The implementation of the DMFT is often simplest on a Bethe lattice with a large coordination number $z \rightarrow \infty$, for which

$$\rho(\epsilon) = \frac{\sqrt{4t^2 - \epsilon^2}}{2\pi t^2} \theta(2t - |\epsilon|). \quad (5)$$

if the bare hopping is normalized as

$$t \rightarrow \frac{t}{\sqrt{z}} \quad (6)$$

We conclude this section by calculating the effective two-body interaction or the low energy scattering amplitude. This will give us a clear idea about the regime of

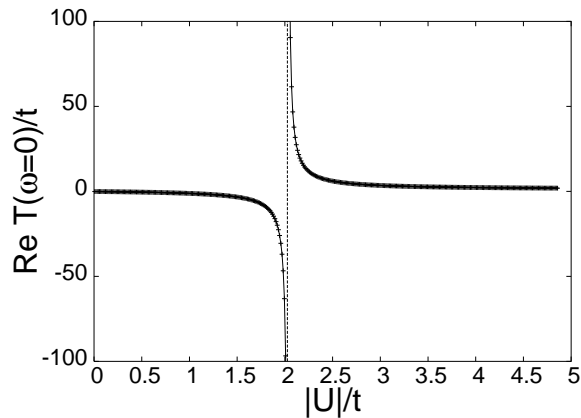


FIG. 1: The real part of the T-matrix $T(\omega \rightarrow 0)$ for the two-body problem is plotted as a function of the attraction $|U|/t$ between two fermions in an otherwise empty Bethe lattice of infinite connectivity. $|U|/t = 2$ is the threshold for the formation of bound state in vacuum.

$|U|/t$ where we expect the corrections to HFB at $T = 0$ to be the most severe, and it will also emphasize the similarity between the continuum Fermi gases often studied theoretically (and now experimentally) and the lattice model studied in this paper. The low energy scattering is described by the real part of the T-matrix $\text{Re}T(\omega \rightarrow 0)$ for the two-body problem in vacuum, i.e., for two fermions in an otherwise empty lattice. This is the analog of the well known three-dimensional “scattering length” for the case of the Bethe lattice studied in this paper. As shown in Fig. 1, for $|U|/t < 2$ the attractive interaction is not sufficient to cause a two-body bound state in vacuum, and $|U|/t = 2$ is the threshold for bound state formation at which the scattering amplitude diverges [14]. We also note that at $|U|/t = 2$ the effective interaction diverges, i.e., one reaches the unitary limit, even though bare $|U|$ is in the intermediate coupling regime. We expect that the deviations from the HFB theory will be maximal in the vicinity of $|U|/t = 2$ where the system is effectively very strongly interacting.

3. DYNAMICAL MEAN FIELD THEORY

To explore the intermediate coupling regime we use the dynamical mean field theory (DMFT) approach [10, 11], which reduces a lattice problem with many degrees of freedom to an effective single-site problem by “integrating out” all the fermionic degrees of freedom except those at one site – the “impurity site” – and retaining the effects of this only in the form of a self-consistently determined bath with which the “impurity site” hybridizes. This retains non-trivial local quantum fluctuations missing in conventional mean field theories and the description can be shown to be exact in the limit of large dimensionality. Since there are many excellent reviews of

DMFT we will only outline the elements of the technique in order to introduce our notation and to indicate the changes in the standard formalism necessitated by the presence of the superconducting long range order.

To take the superconducting order (with singlet pairing) into account we use the Nambu formalism with the spinors $\Psi_k^\dagger \equiv (c_{k\uparrow}^\dagger, c_{-k\downarrow})$ and the matrix Green's function

$$\begin{aligned} \hat{G}(k, \tau) &\equiv -\langle T_\tau \Psi(k, \tau) \Psi^\dagger(k, 0) \rangle \\ &= \begin{pmatrix} G(k, \tau) & F(k, \tau) \\ F^\dagger(k, \tau) & -G(-k, -\tau) \end{pmatrix} \end{aligned} \quad (7)$$

where $F(k, \tau) \equiv -\langle T_\tau c_{k\uparrow}(\tau) c_{-k\downarrow}(0) \rangle$ satisfies $F(-k, -\tau) = F(k, \tau)$. We will denote all Nambu matrices by a 'hat' on top. In this formalism the interaction effects are described in terms of the self energy matrix

$$\hat{\Sigma}(k, i\omega_n) = \begin{pmatrix} \Sigma(k, i\omega_n) & S(k, i\omega_n) \\ S^*(k, -i\omega_n) & -\Sigma^*(k, i\omega_n) \end{pmatrix} \quad (8)$$

where $\omega_n = (2n + 1)\pi/\beta$ are fermionic Matsubara frequencies.

In the limit of infinite dimensions it can be shown that the self energy is *purely local*, i.e., is k independent (see ref. 10), so that $\hat{\Sigma} = \hat{\Sigma}(i\omega_n)$. Furthermore, the SC order parameter can be chosen to be real in a uniform system, which implies that $S(i\omega_n) = S^*(-i\omega_n)$. Hence using the Dyson equation the full Green's function for the lattice can be written as

$$\begin{aligned} \hat{G}^{-1}(k, i\omega_n) &= \begin{pmatrix} i\omega_n + \mu - \epsilon_k & 0 \\ 0 & i\omega_n - \mu + \epsilon_k \end{pmatrix} - \hat{\Sigma}(i\omega_n) \\ &= \begin{pmatrix} i\omega_n + \mu - \epsilon_k - \Sigma(i\omega_n) & -S(i\omega_n) \\ -S(i\omega_n) & i\omega_n - \mu + \epsilon_k + \Sigma(-i\omega_n) \end{pmatrix} \end{aligned} \quad (9)$$

Thus, in DMFT the k -dependence in $\hat{G}^{-1}(k, i\omega_n)$ enters only via the dispersion ϵ_k .

The local self energy is itself obtained from an effective single site problem which can be regarded as arising from integrating out fermionic variables on all sites except one. The effective action for this single site problem within the DMFT approximation is given by

$$\begin{aligned} S_{eff} &= - \int_0^\beta d\tau \int_0^\beta d\tau' \Psi^\dagger(\tau) \hat{\mathcal{G}}^{-1}(\tau - \tau') \Psi(\tau') \\ &\quad - |U| \int_0^\beta d\tau n_\downarrow(\tau) n_\uparrow(\tau). \end{aligned} \quad (10)$$

Here the host (Matrix) Green's function $\hat{\mathcal{G}}$ is *not* the non-interacting local Green's function, as it includes the effects of the fermionic degrees at other sites which have been integrated out *in the presence of interactions*, i.e., it

includes (local) self energy corrections at all these other sites, and needs to be determined by a triangle of self-consistency relations as described below.

The first of these relations comes from the requirement that the "impurity" Green's function for the single site problem should be the same as the local Green's function of the lattice, so that

$$\hat{G}(i\omega_n) = \sum_k \hat{G}(k, i\omega_n). \quad (11)$$

This gives the diagonal and off-diagonal components of the impurity Green's function as

$$G(i\omega_n) = \int_{-\infty}^{\infty} d\epsilon \rho(\epsilon) \frac{\zeta_1 - \epsilon}{(\zeta_1 - \epsilon)(\zeta_2 - \epsilon) + S^2(i\omega_n)}, \quad (12)$$

and

$$F(i\omega_n) = S(i\omega_n) \int_{-\infty}^{\infty} d\epsilon \rho(\epsilon) \frac{1}{(\zeta_1 - \epsilon)(\zeta_2 - \epsilon) + S^2(i\omega_n)} \quad (13)$$

Here $\zeta_1 \equiv i\omega_n + \mu - \Sigma(i\omega_n)$ and $\zeta_2 \equiv i\omega_n + \mu + \Sigma(-i\omega_n)$. For the case of the semi-circular DOS of eq. (5) the integrals can be evaluated in closed form as

$$G(i\omega_n) = \frac{2\zeta_1}{x_1 - x_2} \left[\frac{1}{x_1 + \sqrt{x_1^2 - 4t^2}} - \frac{1}{x_2 + \sqrt{x_2^2 - 4t^2}} \right] \quad (14)$$

$$F(i\omega_n) = \frac{S(i\omega_n)}{x_1 - x_2} \left[\frac{1}{x_1 + \sqrt{x_1^2 - 4t^2}} - \frac{1}{x_2 + \sqrt{x_2^2 - 4t^2}} \right] \quad (15)$$

with $x_{1,2} \equiv \zeta_2 - \zeta_1 \pm \sqrt{(\zeta_2 + \zeta_1)^2 - 4S^2(i\omega_n)}/2$.

The second relation comes from the Dyson equation connecting the full Green's function \hat{G} at the impurity site, the host Green's function $\hat{\mathcal{G}}$ and the self-energy $\hat{\Sigma}$, typically used in reverse, in the form

$$\hat{\mathcal{G}}^{-1}(i\omega_n) = \hat{G}^{-1}(i\omega_n) + \hat{\Sigma}(i\omega_n). \quad (16)$$

The final relation comes from the solution for the self energy of the impurity problem defined by (10), i.e., the determination of

$$\hat{\Sigma}(i\omega_n) = \hat{\Sigma}[\hat{\mathcal{G}}(i\omega_n)] \quad (17)$$

from a knowledge of the host Green's function. This is the task of the "impurity solver", and is typically the hardest step in the triangle of self consistency. In this paper, we use *iterated perturbation theory* (suitably extended to deal with the broken symmetry associated with the superconducting ground state as described in the following section) as the impurity solver.

4. ITERATED PERTURBATION THEORY

We adapt the iterated perturbation theory (IPT), originally developed for the paramagnetic phase of the repulsive Hubbard model [10, 15], to the SC phase of the

attractive Hubbard model. IPT is an approximate technique which is much simpler than the more accurate but elaborate alternate methods such as quantum Monte Carlo [16], exact diagonalization [17], numerical renormalization group [18], local moment approximation [19] etc. IPT gives semi-analytical results which can be directly and easily continued to the real frequency domain. It has been well studied in the context of the DMFT of the Mott transitions in the repulsive Hubbard model [10, 15] where it gives results in complete qualitative agreements with the more accurate methods mentioned above, and only quantitative disagreement typically no more than 10-20 % in the transition temperatures and critical values of U/W ; see, e.g., the comparison of results obtained using different impurity solvers by Bulla et al. [18]. One can reasonably expect similar levels of qualitative and quantitative correctness in the present context in general. If qualitative changes are likely, this is commented on at appropriate places in the paper.

In the form in which we use it here [20], IPT rests on the following ansatz for the self energy as a functional of \hat{G} :

$$\hat{\Sigma}_{IPT}(\omega^+) = \hat{\Sigma}_{HFB} + \hat{A}\hat{\Sigma}^{(2)}(\omega^+). \quad (18)$$

Here $\hat{\Sigma}_{HFB}$ is the Hartree-Fock-Bogoliubov (HFB) self energy as in eq. 19 (see note [21]), $\hat{\Sigma}^{(2)}$ is the second order perturbation theory result (in powers of $|U|$) *but calculated in terms of the Hartree-corrected host Green's function* (see eq. 24), and \hat{A} is to be determined as described below (see eq. 28). All the calculations we report and discuss in this paper are done at $T = 0$, and we work directly in real frequency $\omega^+ = \omega + i0^+$.

The IPT ansatz is constructed so that [20] it

- reproduces the leading order terms for the self energy in the weak coupling limit $|U|/t \ll 1$,
- is exact in the atomic limit $t/|U| = 0$, and
- reproduces the leading order terms for the self energy in the large ω limit for all $|U|/t$, which ensures that some exact sum rules are satisfied.

Thus IPT is expected to provide a reasonable interpolation scheme between the weak and strong coupling limits.

The HFB self energy is given by

$$\hat{\Sigma}_{HF} = -|U|\frac{n}{2}\hat{\tau}_z - \Delta\hat{\tau}_x \quad (19)$$

Here $\hat{\tau}_z$ and $\hat{\tau}_x$ are Pauli matrices in Nambu space. The filling factor $n = \sum_{\sigma} \langle c_{\sigma}^{\dagger} c_{\sigma} \rangle$ and $\Delta = |U|\Phi = |U|\langle c_{\downarrow} c_{\uparrow} \rangle$ with Φ being the superconducting order parameter, are obtained from the full Green's function within IPT as

$$n = -\frac{2}{\pi} \int_{-\infty}^0 \text{Im} G(\omega^+) d\omega \quad (20)$$

$$\Delta = -\frac{|U|}{\pi} \int_{-\infty}^0 \text{Im} F(\omega^+) d\omega \quad (21)$$

The diagonal and off-diagonal components of the second order self energy $\hat{\Sigma}^{(2)}$ are given by

$$\Sigma^{(2)}(t) = -U^2 \left(\tilde{\mathcal{G}}_{11}(t)\tilde{\mathcal{G}}_{22}(-t)\tilde{\mathcal{G}}_{22}(t) - \tilde{\mathcal{F}}_0^{\dagger}(t)\tilde{\mathcal{G}}_{22}(-t)\tilde{\mathcal{F}}_0(t) \right) \quad (22)$$

and

$$S^{(2)}(t) = -U^2 \left(\tilde{\mathcal{F}}_0(t)\tilde{\mathcal{F}}_0(-t)\tilde{\mathcal{F}}_0^{\dagger}(t) - \tilde{\mathcal{G}}_{11}(t)\tilde{\mathcal{F}}_0(-t)\tilde{\mathcal{G}}_{22}(t) \right) \quad (23)$$

Here $\tilde{\mathcal{G}}_{11}$, $\tilde{\mathcal{G}}_{22}$, $\tilde{\mathcal{F}}_0^{\dagger}$ and $\tilde{\mathcal{F}}_0$ are components of the Hartree corrected Host Green's function matrix

$$\begin{pmatrix} \tilde{\mathcal{G}}_{11}(\omega) & \tilde{\mathcal{F}}_0(\omega) \\ \tilde{\mathcal{F}}_0^{\dagger}(\omega) & \tilde{\mathcal{G}}_{22}(\omega) \end{pmatrix}^{-1} = \begin{pmatrix} \mathcal{G}_0(\omega) & \mathcal{F}_0(\omega) \\ \mathcal{F}_0(\omega) & -\mathcal{G}_0^*(-\omega) \end{pmatrix}^{-1} - \hat{\Sigma}_{HFB} \quad (24)$$

The subscript 0 has been added in order to distinguish the components of the host green functions that arise in the specific context of the IPT approximation to the impurity problem.

Each of the terms in (22) and (23) is the product of three factors of the form

$$H(t) = h_1(t)h_2(-t)h_3(t) \quad (25)$$

where each h_i is either $\tilde{\mathcal{G}}_{11}$, $\tilde{\mathcal{G}}_{22}$, $\tilde{\mathcal{F}}_0^{\dagger}$ or $\tilde{\mathcal{F}}_0$. Using the spectral representation for each Green's function we obtain for the Fourier transform,

$$H(\omega^+) = - \int_{-\infty}^{\infty} \prod_{i=1}^3 d\epsilon_i \tilde{\rho}_i(\epsilon_i) \frac{N(\epsilon_1, \epsilon_2, \epsilon_3)}{\omega^+ - \epsilon_1 + \epsilon_2 - \epsilon_3} \quad (26)$$

where $\tilde{\rho}_i(\epsilon_i) = -\text{Im}[h_i(\epsilon_i^+)]/\pi$ and $N(\epsilon_1, \epsilon_2, \epsilon_3)$ is a thermal factor

$$N(\epsilon_1, \epsilon_2, \epsilon_3) = f(\epsilon_1)f(-\epsilon_2)f(\epsilon_3) + f(-\epsilon_1)f(\epsilon_2)f(-\epsilon_3) \quad (27)$$

involving the Fermi function $f(\epsilon) \equiv 1/[1 + \exp(\beta\epsilon)] = 1 - f(-\epsilon)$.

The matrix \hat{A} in (18) is fixed by demanding that $\hat{\Sigma}_{IPT}(\omega^+)$ is "exact" in the large ω limit up to order $1/\omega$. As shown in Appendix A, we find \hat{A} to be proportional to the identity matrix $\hat{\tau}_0$ in Nambu space and given by

$$\hat{A} = \left[\frac{U^2 n_0}{2} \left(1 - \frac{n_0}{2} \right) - \Delta_0^2 \right]^{-1} \left[\frac{U^2 n}{2} \left(1 - \frac{n}{2} \right) - \Delta^2 \right] \hat{\tau}_0 \quad (28)$$

where $\hat{\tau}_0$ is the identity matrix. Here n_0 and Δ_0 denote fictitious "filling factor" and "gap function" values evaluated for the Hartree corrected Host Green's function, i.e.,

$$n_0 = -2/\pi \int_{-\infty}^0 \text{Im} \tilde{\mathcal{G}}_{11}(\omega^+) d\omega \quad (29)$$

and

$$\Delta_0 = -|U|/\pi \int_{-\infty}^0 \text{Im} \tilde{\mathcal{F}}_0(\omega) d\omega. \quad (30)$$

In the atomic limit, as discussed in Appendix B, we find that the second order self energy vanishes. Thus the IPT self energy for $t/U = 0$ is simply the HFB self energy. We show in Appendix B that the HFB result is exact at zero temperature in the broken symmetry phase for $t/U = 0$, and thus our ansatz for the self energy is exact in the atomic limit.

5. RESULTS

We have solved the DMFT equations within the IPT approximation as follows. For a given $|U|/t$ and n , we start with a guess for the self energy $\hat{\Sigma}(\omega^+)$ and the chemical potential μ . With this self energy as input, we compute the full local Green's function $\hat{G}(\omega^+)$ using analytically continued form of eqs. (14) and (15) at $T = 0$. Then we use the Dyson equation (16) to determine the host Green's function \hat{G} . Next we use the IPT ansatz (18-24) to determine the (new) self energy in terms of \hat{G} , using new values of parameters Δ, Δ_0 and n_0 . Finally we obtain the new chemical potential by solving the filling constraint equation (20) using the Broyden method [22]. We then iterate the whole procedure until a self-consistent solution is reached, i.e., convergence in the self energy matrix is achieved.

Within this self-consistency loop the evaluation of n and Δ using eq. (20) and (21) (and similarly for n_0 and Δ_0) involves integrals with singular integrands: the functions $\text{Im} G(\omega^+)$ and $\text{Im} F(\omega^+)$ have square root singularity at a gap edge $\omega = E_g$ which is not a priori known. We fit these functions in a small neighborhood of the gap edge to the form $K/\sqrt{\omega - E_g}$, where the fits determine the gap in the spectrum E_g . Then the singular part of integral near the gap edge is easily evaluated analytically and the part away from the singularity evaluated numerically using Gaussian quadrature.

All of the results reported in this paper have been obtained at a fixed density of $n = 0.5$ (quarter filling) in order to avoid special features that arise at half-filling. (At half-filling, corresponding to $n = 1$, charge density wave order becomes degenerate with SC order and the Hamiltonian has SU(2) symmetry, and is in fact isomorphic to the repulsive Hubbard model which has been well studied within DMFT.) We expect similar results for $n \neq 1$.

Chemical potential: Fig. 2 shows the chemical potential μ tuned to obtain $n = 0.5$ at $T = 0$. We see that it decreases monotonically as a function of $|U|/t$ and the system becomes non-degenerate with increasing attraction between the fermions. For $|U| > 3.5t$ the chemical potential goes below the bottom of the band.

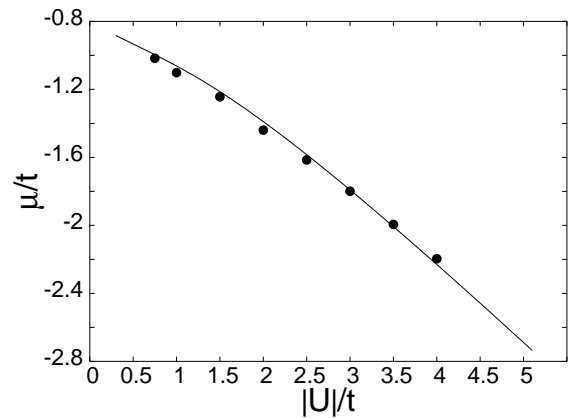


FIG. 2: The chemical potential μ/t as a function of $|U|/t$ for $n = 0.5$ and $T = 0$ within IPT (filled circles) and HFB theory (full line).

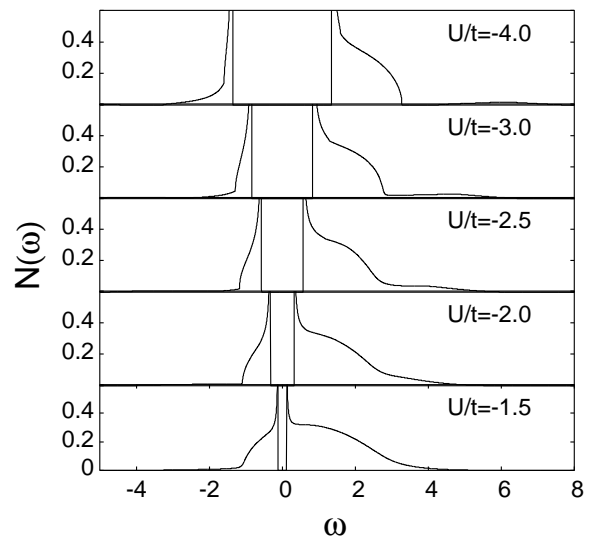


FIG. 3: Single particle density of states (per unit energy per unit area) for $n = 0.5$ and $T = 0$ within IPT for Bethe lattice of infinite connectivity.

Density of states: The single particle density of states (DOS) $N(\omega)$

$$N(\omega) = -\frac{1}{\pi} \text{Im} G(\omega^+) \quad (31)$$

is plotted in Fig. 3 for various values of $|U|/t$. We observe a spectral gap (E_g) in the single particle DOS, which increases with $|U|/t$ as shown in Fig. 4, where the gap as obtained within the HFB theory is also shown for comparison.

For weak coupling the HFB spectral gap has the form $t \exp(-\pi t/2|U|)$, characteristic of BCS theory, while for large attraction it approaches to the binding energy of the composite bosons being proportional to $|U|/2$. The differences of the DMFT result for the energy gap from the simple HFB estimates will be discussed below. Near

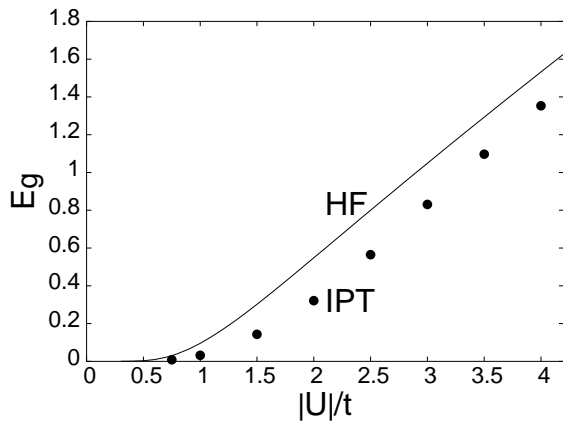


FIG. 4: The spectral gap in the single particle density of states for $n = 0.5$ and $T = 0$ as a function of $|U|/t$ within IPT (filled circles) and HFB theory (full line). Note that the spectral gap within IPT is suppressed as compared to that obtained from HFB theory.

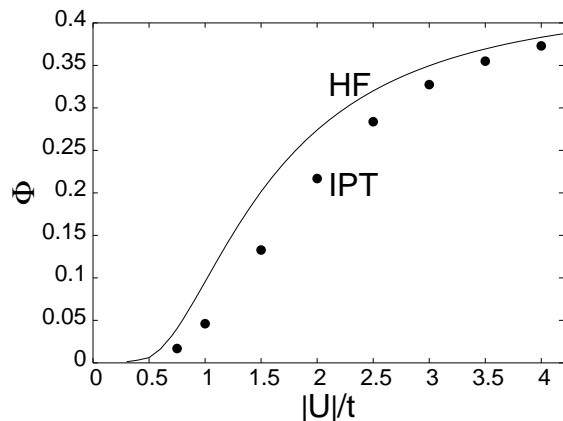


FIG. 5: The superconducting order parameter Φ for $n = 0.5$ and $T = 0$ within IPT (filled circles) and HFB theory (full line). Note that the order parameter within IPT is suppressed as compared to that obtained from HFB theory.

the gap edge the DOS has a square root singularity characteristic of a s-wave superconductor. But the DOS far from the gap edge does not simply look like the non-interacting semi-circular DOS of the Bethe lattice (as would be the case in weak coupling BCS theory). The structure at larger energy values comes from the ω dependence of the self energy, as we discuss below.

Order parameter and energy gap: The superconducting order-parameter is calculated using

$$\Phi = \langle c_{\downarrow} c_{\uparrow} \rangle = -1/\pi \int_{-\infty}^0 \text{Im}F(\omega^+) d\omega$$

and plotted in Fig. 5. We see that, as expected, the quantum fluctuations included in DMFT suppress the order parameter below its HFB mean-field value. The effect of quantum fluctuations in the intermediate coupling regime can be seen more clearly in Fig. 6 where we plot the fractional deviation of DMFT order parameter

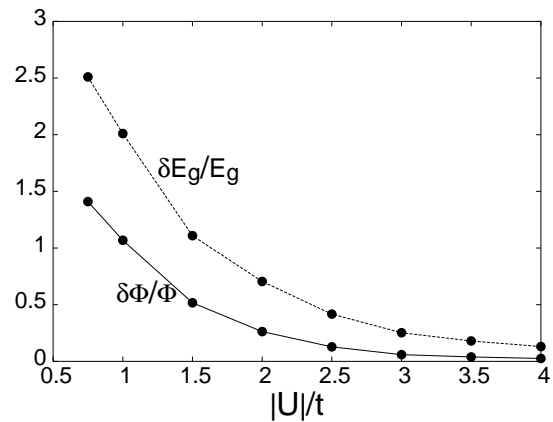


FIG. 6: $\delta\Phi = \Phi_{HFB} - \Phi_{IPT}$ where Φ_{HFB} is the SC order parameter within HFB theory and Φ_{IPT} is the same within IPT. $\delta E_g = (E_g)_{HFB} - (E_g)_{IPT}$ where $(E_g)_{HFB}$ is the spectral gap within HFB theory and $(E_g)_{IPT}$ is the same within IPT.

and the energy gap from their corresponding HFB values. For small to intermediate values of the coupling $U \lesssim t$ the quantitative differences are quite large with the HFB results being larger than the DMFT ones by more than 100%.

Spectral function:

Another important quantity of interest is the one-particle spectral function

$$A(\epsilon, \omega) = -\frac{1}{\pi} \text{Im}G(\epsilon, \omega^+) \quad (32)$$

where G is the “11” component of the Nambu Matrix Green’s function for the lattice obtained by inverting eqn. 9, and is given by

$$G(\epsilon, \omega^+) = \frac{\omega + \epsilon - \mu + \Sigma^*(-\omega^+)}{D(\epsilon, \omega)} \quad (33)$$

with

$$D(\epsilon, \omega) = \quad (34)$$

$$[\omega + \epsilon - \mu + \Sigma^*(-\omega^+)] [\omega - \epsilon + \mu - \Sigma(\omega^+)] - S^2(\omega^+)$$

Since we are working within the DMFT framework, we have traded the \mathbf{k} label for the energy label ϵ .

Quite generally, we expect that the spectral function will be of the form

$$A(\epsilon, \omega) = Z_+(\epsilon)\delta(\omega - E) + Z_-(\epsilon)\delta(\omega + E) + A_{inc}(\epsilon, \omega) \quad (35)$$

where $Z_{\pm}(\epsilon)$ are the coherent spectral weights in the Bogoliubov quasiparticle/quasihole excitation poles at energies $\pm E(\epsilon)$, and A_{inc} is the incoherent part of the spectral function. We recall that in simple BCS-HFB mean field theory $Z_{\pm} = (1 \pm \xi/E)/2$ where $\xi = \epsilon - \mu - |U|n/2$ and $E = \sqrt{\xi^2 + \Delta^2}$ and $A_{inc} = 0$. In contrast, as shown in

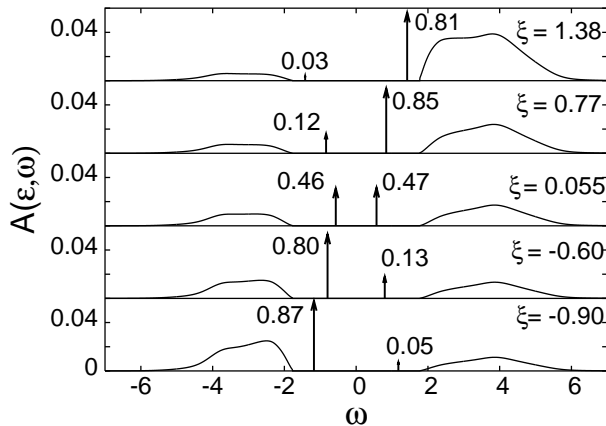


FIG. 7: The spectral function $A(\epsilon, \omega)$ for $n = 0.5$, $T = 0$ and $|U| = 2.5t$ as a function of ω for various values of $\xi = \epsilon - \mu + \Sigma'(\omega = E)$. Note that $A(\epsilon, \omega)$ not only has coherent delta function peaks (which are shown by arrows with the corresponding weights) but also has broad incoherent parts which start appearing for $\omega \geq 3E_g$. For $|U| = 2.5t$, $E_g = 0.57t$.

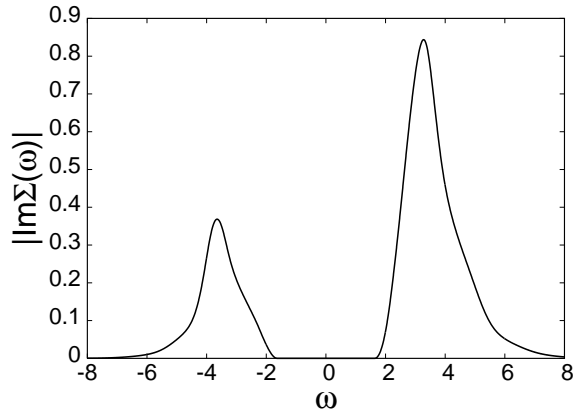


FIG. 8: The imaginary part of self energy $|\Sigma''(\omega)|$ for $n = 0.5$, $T = 0$ and $|U|/t = 2.5$ as a function of ω . Note that $|\Sigma''(\omega)|$ becomes non-zero only for $\omega \geq 3E_g$. For $|U| = 2.5t$, $E_g = 0.57t$.

Fig. 7 the DMFT result for $A(\epsilon, \omega)$ not only has sharp delta function peaks at $\pm E$ corresponding to the Bogoliubov excitations but also has a broad incoherent part. The weight in the coherent excitations $Z_+ + Z_- < 1$ and the deficit from unity is contained in A_{inc} . All of this is a consequence of the frequency dependent self-energy as shown below.

The imaginary part of the (diagonal) self energy is plotted in Fig. 8. It vanishes at low energies ($|\omega| < 3E_g$) since there are no final states available for a scattering event. In this regime, from eqs. (32) and (33) it follows that

$$A(\epsilon, \omega) = (\omega + \epsilon - \mu + \Sigma(-\omega)) \delta(D(\epsilon, \omega)), \quad (36)$$

with $D(\epsilon, \omega) = (\omega + \epsilon - \mu + \Sigma(-\omega))(\omega - \epsilon + \mu - \Sigma(\omega)) - S^2(\omega)$, since $\Sigma(\omega)$ and $S(\omega)$ are now real. The quasipar-

ticle excitation energies are the two symmetrically placed zeros at $\omega = \pm E$ of D which is an even function of ω . Thus the excitation energies are given by

$$D(\epsilon, \pm E) = 0. \quad (37)$$

and the residues at the Bogoliubov quasiparticle poles are then reduced compared to their HFB values and are given by

$$Z_{\pm}(\epsilon) = [\pm E + \epsilon - \mu + \Sigma(\mp E)] \left/ \left| \frac{\partial D}{\partial \omega}(\omega = \pm E) \right| \right. \quad (38)$$

The imaginary part of the (diagonal) self energy becomes non-zero for $\omega \geq 3E_g$ as shown in Fig. 8. This can be seen to arise from the form of the second order self energy of eq. (22), because in a system with a gap, final states for scattering an injected particle off a particle-hole pair are available only if incident particle has $\omega \geq 3E_g$. We should note, however, that the $3E_g$ value of the threshold is likely an artifact of DMFT/IPT which ignores collective excitations. It is well known [13] that in finite dimensions this model has a linearly dispersing sound mode and scattering of a one-particle excitation off such a collective mode should lead to non-zero $\text{Im}\Sigma(\omega)$ above E_g and not $3E_g$.

In any case, within IPT, the structure of the self energy leads to the incoherent spectral weight in $A(\epsilon, \omega)$ above three times the gap. The reduction of the coherent quasiparticle weight and the transfer of spectral weight to the incoherent part of the spectral function are thus features related to the ω dependent self energy and are missing in simple HFB mean field theory.

Occupation probability: We next calculate the analog of the momentum distribution within the DMFT, namely the occupation probability $n(\epsilon)$ of an energy level ϵ given by

$$n(\epsilon) = \int_{-\infty}^0 A(\epsilon, \omega) d\omega. \quad (39)$$

This is plotted in Fig. 9 for various values of $|U|/t$.

Within the HFB approximation, $n(\epsilon)$ has the following simple form:

$$n(\epsilon) = Z_-(\epsilon) = \frac{1}{2} \left(1 - \frac{\xi}{E} \right) \quad (40)$$

It is easy to see that in the weak coupling limit $n(\epsilon)$ looks like a slightly broadened Fermi function, dropping from 1 to zero over an energy scale of order Δ ; its width hence increases monotonically with $|U|/t$. As one begins to form more and more tightly bound pairs, higher ϵ states need to be involved in the pairing and eventually the system becomes non degenerate even at $T = 0$ as already argued from the chemical potential. Note that $n(\epsilon)$ within IPT is always less rounded than that within

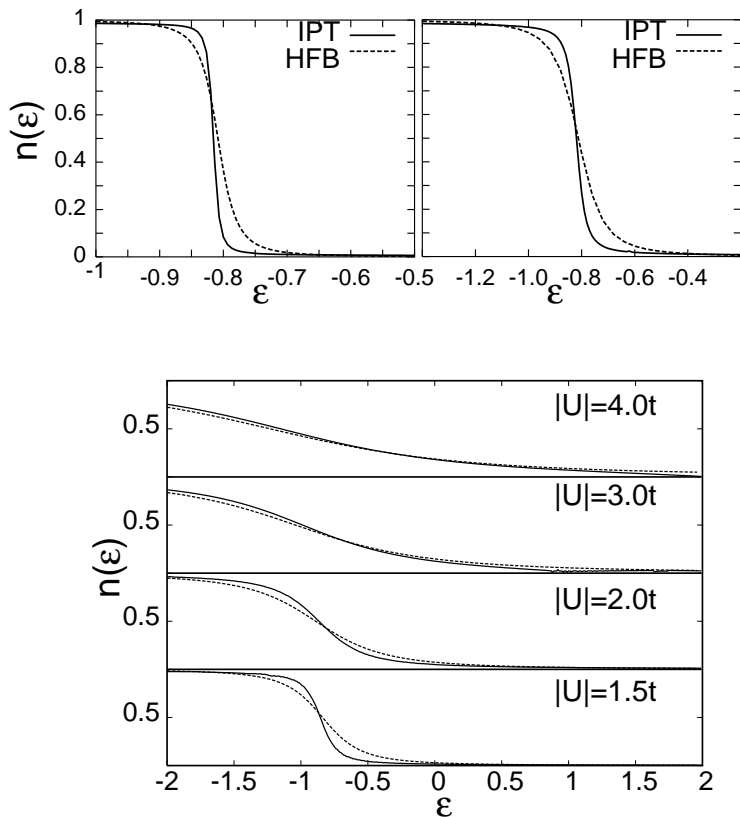


FIG. 9: The occupation probability $n(\epsilon)$ of an energy level ϵ for $n = 0.5$, $T = 0$ for various values of $|U|/t$ obtained within IPT (full curve) and HFB approximation (dashed curve). Top right panel shows $n(\epsilon)$ for $|U| = 0.75t$ and top left panel shows $n(\epsilon)$ for $|U| = 1.0t$. Note ϵ scale over which these are plotted are different. Bottom panel shows $n(\epsilon)$ for $|U| = 1.5t, 2.0t, 3.0t$ and $4.0t$ starting from bottom to top.

HFB because quantum fluctuations reduce the gap in the single particle dos relative to HFB value.

We find that the exact sum rule $\int_{-\infty}^{\infty} n(\epsilon)\rho_0(\epsilon)d\epsilon = n/2$ is satisfied in our IPT calculation within the estimated numerical errors (0.4% – 2%).

Superfluid stiffness: We can also estimate an upper bound on the superfluid stiffness D_s which is the strength of the delta function in the real part of optical conductivity :

$$\text{Re}\sigma(\omega) = D_s\delta(\omega) + \text{Re}\sigma_{reg}(\omega), \quad (41)$$

The Kubo formula for the superfluid stiffness [23] can be written as

$$\frac{D_s}{\pi} = -\langle\mathcal{K}_x\rangle - \text{Re}\Lambda_T(q_x = 0, q_y \rightarrow 0, \omega = 0) \quad (42)$$

where the kinetic energy $-\langle\mathcal{K}_x\rangle$ is the diamagnetic response of the system to the vector potential and the transverse current-current correlation function Λ_T is the paramagnetic response. It is easy to see that $\Lambda_T \geq 0$, so that $D_s \leq \pi|\langle\mathcal{K}_x\rangle|$. Thus the the kinetic energy gives an

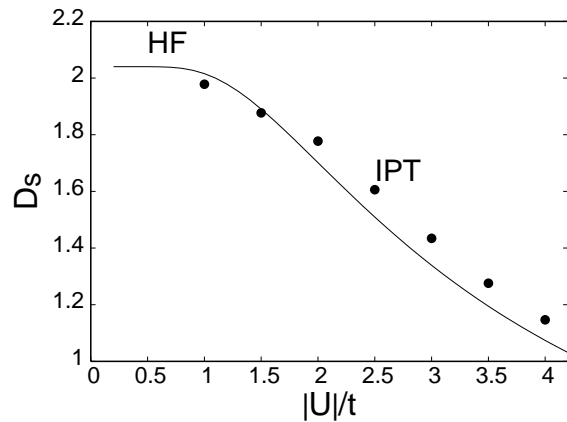


FIG. 10: Upper bound on the superfluid stiffness D_s for $n = 0.5$, $T = 0$ as a function of the coupling constant $|U|/t$ within IPT (filled circles) and HFB theory (full line).

upper bound to the superfluid stiffness, and in fact we may use it to provide a rough estimate of D_s (although, as emphasized in ref. [24], there is no reason to assume in general that for a lattice model D_s is identical to $\pi|\langle\mathcal{K}_x\rangle|$ even though this equality holds within simple BCS-HFB theory.) In Fig. 10 we plot the superfluid stiffness D_s as a function of the attractive interaction. We find that it is of order t in weak coupling, but decreases monotonically with $|U|/t$ reaching $\sim t^2/|U|$ in the strong coupling limit, which reflects the increasing effective mass of the hard core lattice bosons in the large $|U|$ limit.

6. CONCLUSIONS

In this paper we have studied the crossover from BCS superconductivity to BEC at $T = 0$ in the attractive Hubbard model using dynamical mean field theory (DMFT), implemented using the iterated perturbation theory (IPT) scheme. Our main goal was to explore the DMFT approach in a broken symmetry state, which has received less attention than the paramagnetic phase, within a simple, easily implemented, semi-analytic scheme, and to see how the quantum fluctuations included in this framework modify the Hartree-Fock-Bogoliubov (HFB) mean field results. For the most part we found that HFB is qualitatively correct but overestimates the SC order parameter and energy gap. In the intermediate coupling regime, the quantitative changes can be quite large. The frequency dependent self-energy of DMFT leads to the appearance of incoherent contributions to the single particle spectral function at energies larger than three times the gap, and the consequent reduction in the coherent spectral weight in the Bogoliubov quasiparticle/quasihole poles in the spectrum .

ACKNOWLEDGMENTS

A. G. would like to thank S.R. Hassan and R. Karan for many useful discussions and acknowledge the hospitality of the Department of Physics, I.I.Sc., Bangalore, over a period during which a part of this work was done. M.R.'s work at TIFR was supported in part by the Department of Science and Technology under a Swarnajayanti Grant.

APPENDIX A : LARGE ω LIMIT

In this Appendix we will first determine the large ω limit of the self energy and then use it to fix the parameter \hat{A} in our IPT ansatz (18). The $\omega \rightarrow \infty$ limit can be obtained by a moment expansion of the Green's function

$$G(\omega^+) = \frac{1}{\omega^+} \left[M^{(0)} + \frac{M^{(1)}}{\omega} + \frac{M^{(2)}}{\omega^2} + \dots \right], \quad (43)$$

which follows from the spectral representation

$$G(\omega^+) = \int_{-\infty}^{\infty} \frac{\rho_G(\epsilon) d\epsilon}{\omega^+ - \epsilon} \quad (44)$$

and the definition of the n^{th} moment of the density of states $M^{(n)} = \int_{-\infty}^{\infty} \rho_G(\omega) \omega^n d\omega$.

To evaluate the moments it is useful to go to a Hamiltonian formulation for single site impurity problem, which requires introducing auxiliary degrees of freedom to describe the "bath". For the superconducting phase of the negative U Hubbard model, one possible choice for the impurity Hamiltonian is :

$$\begin{aligned} H_{imp} = & -\mu \sum_{\sigma} c_{\sigma}^{\dagger} c_{\sigma} - |U| n_{\uparrow} n_{\downarrow} + \sum_{k\sigma} \epsilon_k f_{k\sigma}^{\dagger} f_{k\sigma} \\ & + \sum_{k\sigma} V_k \left(c_{\sigma}^{\dagger} f_{k\sigma} + f_{k\sigma}^{\dagger} c_{\sigma} \right) + D \sum_k \left(f_{k\uparrow}^{\dagger} f_{-k\downarrow}^{\dagger} + f_{-k\downarrow} f_{k\uparrow} \right) \end{aligned} \quad (45)$$

which describes the impurity c_{σ} coupled to superconducting bath of f fermions. Here V_k is the hybridization parameter which allows fermions to hop between the bath and the impurity site and the D term represents s-wave pairing of the f 's.

Using the spectral representation, the moments can be written in terms of commutators ($[,]$) and anticommutators ($\{, \}$) involving the c 's and the impurity Hamiltonian:

$$\hat{M}_{\alpha\beta}^{(0)} = \langle \{ c_{\alpha}, c_{\beta}^{\dagger} \} \rangle = \delta_{\alpha\beta} \quad (46)$$

$$\hat{M}_{\alpha\beta}^{(1)} = \langle \{ [c_{\alpha}, H_{imp}], c_{\beta}^{\dagger} \} \rangle \quad (47)$$

and

$$\hat{M}_{\alpha\beta}^{(2)} = \langle \{ [[c_{\alpha}, H_{imp}], H_{imp}] c_{\beta}^{\dagger} \} \rangle \quad (48)$$

where $\alpha, \beta = \uparrow, \downarrow$. Explicit evaluation of these commutators leads to the results

$$\hat{M}^{(1)} = (-\mu - |U|n/2)\hat{\tau}_z + \Delta\hat{\tau}_x \quad (49)$$

$$\hat{M}^{(2)} = \left[\mu^2 + \frac{(2\mu|U| + U^2)n}{2} \right] \hat{\tau}_0 \quad (50)$$

The Host Green's function $\hat{\mathcal{G}}$ is obtained from the impurity Hamiltonian setting $U = 0$, and its large ω limit is

$$\hat{\mathcal{G}}^{-1}(\omega^+) \simeq \omega^+ \hat{\tau}_0 + (\mu - \sum_k V_k^2/\omega) \hat{\tau}_z \quad (51)$$

Using the Dyson equation, the large ω limit of self energy is then found to be

$$\hat{\Sigma}(\omega^+) = \hat{\Sigma}_{HFB} + \frac{U^2 n(1-n/2)/2 - \Delta^2}{\omega^+} \hat{\tau}_0. \quad (52)$$

We must now find the large ω limit of IPT self energy, and compare it with the exact $\omega \rightarrow \infty$ result (52) derived above. Begin with the diagonal component of $\hat{\Sigma}^{(2)}(\omega)$ given by

$$\Sigma^{(2)}(\omega^+) = U^2 \int_{-\infty}^{\infty} \prod_{i=1}^3 d\epsilon_i \frac{g_1(\epsilon_1, \epsilon_2, \epsilon_3) N(\epsilon_1, \epsilon_2, \epsilon_3)}{\omega^+ - \epsilon_1 + \epsilon_2 - \epsilon_3} \quad (53)$$

where

$$g_1(\epsilon_1, \epsilon_2, \epsilon_3) = \tilde{\rho}_{11}(\epsilon_1) \tilde{\rho}_{22}(\epsilon_2) \tilde{\rho}_{22}(\epsilon_3) - \tilde{\rho}_f(\epsilon_1) \tilde{\rho}_{22}(\epsilon_2) \tilde{\rho}_f(\epsilon_3) \quad (54)$$

Here $\tilde{\rho}_{ii}(\omega) = -1/\pi \text{Im } \tilde{\mathcal{G}}_{ii}(\omega^+)$ with $i = 1, 2$ and $\tilde{\rho}_f(\omega) = -1/\pi \text{Im } \tilde{\mathcal{F}}_0(\omega^+)$. In the large ω limit it suffices to keep terms up to order $1/\omega$. We thus get

$$\Sigma^{(2)}(\omega^+) \simeq \frac{1}{\omega^+} \left[\frac{U^2 n_0}{2} \left(1 - \frac{n_0}{2} \right) - \Delta_0^2 \right] \quad (55)$$

Next, consider the off-diagonal component of $\hat{\Sigma}^{(2)}(\omega)$

$$S^{(2)}(\omega^+) = U^2 \int_{-\infty}^{\infty} \prod_{i=1}^3 d\epsilon_i \frac{g_2(\epsilon_1, \epsilon_2, \epsilon_3) N(\epsilon_1, \epsilon_2, \epsilon_3)}{\omega^+ - \epsilon_1 + \epsilon_2 - \epsilon_3} \quad (56)$$

where

$$g_2(\epsilon_1, \epsilon_2, \epsilon_3) = \tilde{\rho}_f(\epsilon_1) \tilde{\rho}_f(\epsilon_2) \tilde{\rho}_f(\epsilon_3) - \tilde{\rho}_{11}(\epsilon_1) \tilde{\rho}_f(\epsilon_2) \tilde{\rho}_{22}(\epsilon_3) \quad (57)$$

It is easy to check that in the large ω limit $S^{(2)}$ vanishes up to order $1/\omega$.

Comparing the large ω limits of the IPT ansatz $\hat{\Sigma}_{HFB} + \hat{A} \hat{\Sigma}^{(2)}(\omega)$ and the exact self energy (52), we find

$$\hat{A} = \left[\frac{U^2 n_0}{2} \left(1 - \frac{n_0}{2} \right) - \Delta_0^2 \right]^{-1} \left[\frac{U^2 n}{2} \left(1 - \frac{n}{2} \right) - \Delta^2 \right] \hat{\tau}_0 \quad (58)$$

APPENDIX B : ATOMIC LIMIT

In this Appendix first we first solve the attractive Hubbard model exactly in the atomic limit $t/U = 0$ and then show that our IPT ansatz for self energy is exact in this limit. In the atomic limit one can drop the hopping term in the Hubbard Hamiltonian (and also the hybridization term in the impurity Hamiltonian) so that

$$H = -|U|n_{\uparrow}n_{\downarrow} - \mu(n_{\uparrow} + n_{\downarrow}) \quad (59)$$

The various sites decouple and so we have dropped the site label. The four states are $|0\rangle, |\uparrow\rangle, |\downarrow\rangle$ and $|\uparrow\downarrow\rangle$ with corresponding energies $0, -\mu, -\mu$ and $-2\mu - |U|$.

To study the broken symmetry phase we introduce a pairing field h ,

$$H = -|U|n_{\uparrow}n_{\downarrow} - \mu(n_{\uparrow} + n_{\downarrow}) - h(c_{\uparrow}^{\dagger}c_{\downarrow}^{\dagger} + c_{\downarrow}c_{\uparrow}) \quad (60)$$

and finally take the $h \rightarrow 0$ limit. The $T = 0$ equations for the filling factor and order parameter are given by

$$n = \frac{2}{1 + (h/\lambda)^2} \text{ and } \Delta = \frac{-|U|h/\lambda}{1 + (h/\lambda)^2} \quad (61)$$

where $\lambda = (-(2\mu + |U|) - \sqrt{(2\mu + |U|)^2 + 4h^2})/2$ is the lowest eigenvalue of the Hamiltonian. We thus find that in the $h \rightarrow 0$ limit we get the atomic limit solution: $\mu = -|U|/2$ for any filling n and $\Delta = |U|\sqrt{n(2-n)}/2$.

Now consider the HFB equations in the atomic limit at $T = 0$

$$n = 2 \left[1 + \frac{\mu + |U|n/2}{\sqrt{(\mu + |U|n/2)^2 + \Delta^2}} \right] \quad (62)$$

and

$$\frac{1}{|U|} = \frac{1}{2\sqrt{(\mu + |U|n/2)^2 + \Delta^2}} \quad (63)$$

The solution of these self consistent equations is $\mu = -|U|/2$ and $\Delta = |U|\sqrt{n(2-n)}/2$, which shows that HFB theory is exact in the atomic limit at zero temperature.

Finally we will show that the second order self energy vanishes in the atomic limit. The Hartree corrected Host Green's function

$$\hat{\mathcal{G}}^{-1}(w^+) = \hat{\mathcal{G}}^{-1}(w^+) - \hat{\Sigma}_{HFB} \quad (64)$$

reduces in the atomic limit to

$$\hat{\mathcal{G}}^{-1}(w^+) = w^+ \hat{\tau}_0 + (\mu + |U|n/2) \hat{\tau}_z + \Delta \hat{\tau}_x \quad (65)$$

It can be checked that the full Green's function in the atomic limit is identical to this, which means that $\hat{\Sigma}^{(2)}(\omega)$ vanishes. Alternatively one can calculate the density of states corresponding to $\hat{\mathcal{G}}_0$, which are given by

$$\tilde{\rho}_{11}(w) = (1-n/2)\delta(w-|U|/2) + (n/2)\delta(w+|U|/2) = \tilde{\rho}_{22}(-w) \quad (66)$$

and

$$\tilde{\rho}_f(w) = -\Delta/|U|(\delta(w - |U|/2) - \delta(w + |U|/2)) \quad (67)$$

and substitute these in the expression for the $\hat{\Sigma}^{(2)}(\omega)$ and check that all the components of second order self energy matrix vanish in the atomic limit.

-
- [1] D. M. Eagles, Phys. Rev. **186**, 456 (1969).
 - [2] A. J. Leggett in *Modern Trends in the Theory of Condensed Matter*, A. Pekalski and R. Przystawa, eds. (Springer-Verlag, Berlin, 1980); and J. Phys. (Paris) Colloq. **41**, C7-19 (1980).
 - [3] P. Nozières and S. Schmitt-Rink, J. Low temp. Phys. **59**, 195 (1985).
 - [4] For a review, see M. Randeria in *Bose-Einstein Condensation*, edited by A. Griffin, D. Snoke, and S. Stringari, (Cambridge University Press, Cambridge, England, 1994).
 - [5] M. Randeria, J. M. Duan, and L. Y. Shieh, Phys. Rev. Lett. **62**, 981 (1989) and Phys. Rev. B, **41**, 327 (1990).
 - [6] C. A. R. Sá de Melo, M. Randeria, and J. R. Engelbrecht, Phys. Rev. Lett. **71**, 3202 (1993); J. R. Engelbrecht, M. Randeria, and C. A. R. Sá de Melo, Phys. Rev. B **55**, 15,153 (1997).
 - [7] M. Randeria, N. Trivedi, A. Moreo, and R. T. Scalettar, Phys. Rev. Lett. **69**, 2001 (1992).
 - [8] N. Trivedi and M. Randeria, Phys. Rev. Lett. **75**, 312 (1995).
 - [9] S. Jochim, M. Bartenstein, A. Altmeyer, G. Hendl, S. Riedl, C. Chin, J. H. Denschlag, and R. Grimm, Science **302**, 2101-2103 (2003), M. Bartenstein, A. Altmeyer, S. Riedl, S. Jochim, C. Chin, J. H. Denschlag, and R. Grimm, Phys. Rev. Lett. **92**, 120401 (2004) and Phys. Rev. Lett. **92**, 203201 (2004), C. A. Regal, M. Greiner, and D. S. Jin, Phys. Rev. Lett, **92**, 040403 (2004) and condmat/0311172, M. Greiner, C. A. Regal, and D. S. Jin, Nature **426**, 537 (2003), M. W. Zwierlein, C. A. Stan, C. H. Schunck, S. M. F. Raupach, S. Gupta, Z. Hadzibabic, and W. Ketterle, Phys. Rev. Lett. **91**, 250401 (2003), Z. Hadzibabic, S. Gupta, C. A. Stan, C. H. Schunck, M. W. Zwierlein, K. Dieckmann, and W. Ketterle, Phys. Rev. Lett. **91**, 160401 (2003), S. Gupta, Z. Hadzibabic, M. W. Zwierlein, C. A. Stan, K. Dieckmann, C. H. Schunck, E. G. M. van Kempen, B. J. Verhaar, and W. Ketterle, Science **300**, 1723-1726 (2003), M. W. Zwierlein, C. A. Stan, C. H. Schunck, S. M. F. Raupach, A. J. Kerman, and W. Ketterle, Phys. Rev. Lett. **92**, 120403 (2004).
 - [10] A. Georges, G. Kotliar, W. Krauth, and M.J. Rozenberg, Rev. Mod. Phys. **68**, 13 (1996).
 - [11] T. Pruschke, M. Jarrell, and J. K. Freericks, Adv. Phys. **44**, 187 (1995).
 - [12] M. Keller, W. Metzner, and U. Schollwock, Phys. Rev. B, **60**, 3499 (1999), Phys. Rev. Lett. **86**, 4612 (2001) and condmat/0109343, M. Capone, C. Castellani, and M. Grilli, Phys. Rev. Lett. **88**, 126403 (2002).

- [13] L. Belkhir and M. Randeria, Phys. Rev. B **49**, 6829 (1994).
- [14] *Modern Quantum Mechanics* by J. J. Sakurai chapter 7 eds. (Pearson Educations, 1999).
- [15] H. Kajueter and G. Kotliar, Phys. Rev. Lett. **77**, 131 (1996).
- [16] M. Jarrell, Phys. Rev. Lett. **69**, 168 (1992), M. J. Rozenberg, X. Y. Zhang, and G. Kotliar, Phys. Rev. Lett. **69**, 1236 (1992), A. Georges and W. Krauth, Phys. Rev. Lett. **69**, 1240 (1992).
- [17] M. Caffarel and W. Krauth, Phys. Rev. Lett. **72**, 1545 (1994), M. J. Rozenberg, G. Moeller, and G. Kotliar, Mod. Phys. Lett. **8**, 535 (1994), Q. Si, M. J. Rozenberg, G. Kotliar and A. E. Ruckenstein, Phys. Rev. Lett. **72**, 2761 (1994).
- [18] K. G. Wilson, Rev. Mod. Phys. **47**, 773 (1975), H. R. Krishna-murthy, J. W. Wilkins, and K. G. Wilson, Phys. Rev. B **21**, 1003 (1980), O. Sakai, Y. Kumamoto, Solid State Commun. **89**, 307 (1994), R. Bulla, A. C. Hewson, and Th. Pruschke, J. Phys. Condens. Matter **10**, 8365 (1998), R. Bulla, T. A. Costi, and D. Vollhardt, Phys. Rev. B **64**, 045103 (2001), D. Meyer, A. C. Hewson, and R. Bulla, Phys. Rev. Lett. **89**, 196401 (2002)
- [19] D. E. Logan, M. P. Eastwood, and M. A. Tusch, J. Phys. Condens. Matter **10**, 2673 (1998), N. L. Dickens and D. E. Logan, J. Phys. Condens. Matter **13**, 4505 (2001), D. E. Logan and N. L. Dickens, J. Phys. Condens. Matter **13**, 9713 (2001), D. E. Logan and N. L. Dickens, J. Phys. Condens. Matter **14**, 3605 (2002), V. E. Smith, D. E. Logan, and H. R. Krishnamurthy, condmat/0303229, N. S. Vidhyadhiraja, V. E. Smith, D. E. Logan, and H. R. Krishnamurthy, condmat/0307462.
- [20] Note that we do not impose the Luttinger Integral Theorem (also refereed to as the Luttinger sum rule). While its imposition is of importance in metallic systems to ensure Fermi liquid properties [10, 15], we believe that its importance is not as crucial in gapped systems such as the ones under discussion.
- [21] We note that in the presence of the IPT contributions to the self energy, the values of μ and Δ , obtained from eqs. (21,20), are different from the values that arise in pure HFB.
- [22] *Numerical Recipes in Fortran* by W. H. Press, S. A. Teukolsky, W. T. Vetterling, and B. P. Flannery page **382**, chapter **9** eds. (Cambridge University Press, 1993).
- [23] D. J. Scalapino, S. R. White, and S. Zhang, Phys. Rev. B, **47**, 7995 (1993).
- [24] A. Paramekanti, N. Trivedi, and M. Randeria, Phys. Rev. B **57**, 11639 (1998).